

Earthquake Response Analysis of a Gravity Dam Considering the Radiation

Damping of Infinite Foundation

* Y.S. Liu¹ and D.H. Chen²

¹College of Hydraulic & Environmental Engineering, China Three Gorges University, China

²College of Civil Engineering & Architecture, China Three Gorges University, China

*Corresponding author:ys850728@126.com

Abstract

Two different earthquake input models are presented in the paper, i.e. massless foundation model and viscous-spring boundary. Based on the commercial nonlinear finite element code ANSYS, the user element subroutine of the viscous-spring boundary is implemented. The correctness of the viscous-spring boundary and its wave input model are validated by a numerical example. Finally, the viscous-spring boundary and wave input model are applied to the seismic analysis of the Longtan gravity dam-foundation system. The results show that the peak values of dam's dynamic responses are reduced by 4%~38% compared to the massless foundation model. The structural dynamic responses are overestimated to some extent utilizing the traditional massless model. The radiation damping effect of infinite foundation has a great influence to the structure's dynamic responses, and is very necessary to be considered.

Keywords: Dam-foundation dynamic interaction; Viscous-spring boundary; Wave input model; Longtan gravity dam

Introduction

Dam-foundation dynamic interaction and the earthquake input mechanism are the key issues of safety evaluation of high dams. Clough (1980) proposed a massless foundation model and assumed that the foundation is linear elastic, massless, and the earthquake excitations act uniformly on the truncated boundary. It has been widely used in the practical engineering studies. But this model still has some limitations, which include: (1) The foundation is actually a mass of semi-infinite medium. The seismic wave energy will be dissipated to infinity. The infinite foundation plays a role in the absorption of the scattering seismic wave energy. (2) The high dams are usually built in narrow mountain valleys. There are apparent differences of the amplitude and phase of the earthquake along the interface of the dam foundation. It is difficult to reflect actual seismic responses for high dams when the ununiform earthquake excitations are neglected.

Many studies have been made to study the dam-foundation dynamic interaction. These include the viscous boundary (Lysmer and Kuhlemeyer, 1969), the viscous-spring boundary (Deeks and Randolph, 1994; Liu *et al.*, 2006), the transmitting boundary (Liao *et al.*, 1984), and the scaled boundary finite element method (Wolf and Song, 1996). The viscous-spring boundary is very efficient and convenient to incorporate it with the commercial finite element software and has sufficient accuracy without much increasing computational efforts.

This paper is organized as follows. Section 2 describes a viscous-spring boundary element and its seismic input model. Section 3 presents a numerical example to validate the correctness of the programme. Section 4 demonstrates the application of the proposed coupled method to the seismic analysis of the Longtan gravity dam-foundation system. Section 5 summarizes some major conclusions from this contribution.

Viscous-spring boundary element and its seismic input model

Viscous-spring boundary condition

A 2-D viscous-spring boundary is employed to absorb the wave energy radiating away from the dam. A sketch of the viscous-spring boundary used in the gravity dam-foundation system and the parallel-connected spring-dashpot system in each direction is shown in Fig. 1. The normal and tangential spring and damping coefficients (Du *et al.*, 2006) of the viscous-spring boundary are taken as

$$\begin{cases} K_{BN} = \frac{1}{1+\alpha} \frac{\lambda+2G}{2r_b}, C_{BN} = \beta\rho c_p \\ K_{BT} = \frac{1}{1+\alpha} \frac{G}{2r_b}, C_{BT} = \beta\rho c_s \end{cases} \quad (1)$$

where K_{BN} and K_{BT} are the normal and tangential stiffness coefficients, respectively. C_{BN} and C_{BT} are the normal and tangential damping coefficients, respectively. A is the total area of all elements around a node at the boundary. r_b is the distance from the scattering wave source to the artificial boundary point. c_s and c_p are the wave velocities of the S wave and P wave, respectively. G and ρ denote the medium's shear modulus and mass density, respectively. α and β are dimensionless parameters, and are taken as 0.8 and 1.1, respectively (Du *et al.*, 2006).

The viscous-spring boundary is a continuous stress boundary that can be discretized with a common shape function. The shape function at the node i is

$$N_i(x) = 1 - \frac{x}{l}, \quad N_j(x) = \frac{x}{l} \quad (2)$$

The shape function for the displacements is expressed as

$$[N] = \begin{bmatrix} N_i(x) & 0 & N_j(x) & 0 \\ 0 & N_i(x) & 0 & N_j(x) \end{bmatrix} \quad (3)$$

The elastic matrix is taken as

$$[D] = \begin{bmatrix} K_{BT} & 0 \\ 0 & K_{BN} \end{bmatrix} \quad (4)$$

The stiffness matrix of a viscous-spring element is calculated using Eq. (5)

$$[K] = \int_0^l [N]^T [D] [N] dx dy \quad (5)$$

Thus, the stiffness matrix of the viscous-spring element is shown in Eq. (6)

$$[K]_B = \frac{l}{6} \begin{bmatrix} 2K_{BT} & 0 & K_{BT} & 0 \\ & 2K_{BN} & 0 & K_{BN} \\ & & 2K_{BT} & 0 \\ sym & & & 2K_{BN} \end{bmatrix} \quad (6)$$

where l is the length of a viscous-spring boundary element. The damping matrix $[C]_B$ has a similar form and is constructed from $[K]_B$ by replacing K with C .

The free field input model

The earthquake free field motions with viscous-spring elements can be translated into equivalent force loads at the truncated boundary of dam-foundation system using Eq. (7).

$$\mathbf{F}_B = \mathbf{K}_B \mathbf{u}_B^f + \mathbf{C}_B \dot{\mathbf{u}}_B^f + \boldsymbol{\sigma}_B^f \mathbf{n} \quad (7)$$

In Eq. (7), the subscript B denotes a boundary node at the viscous-spring boundary. K_B and C_B are the spring and damping coefficients, respectively, which are described in Eq. (1). u_B^f and \dot{u}_B^f are the free field displacement and velocity, respectively. σ_B^f is the free field stress and \mathbf{n} is outward normal direction cosine of the free field boundary.

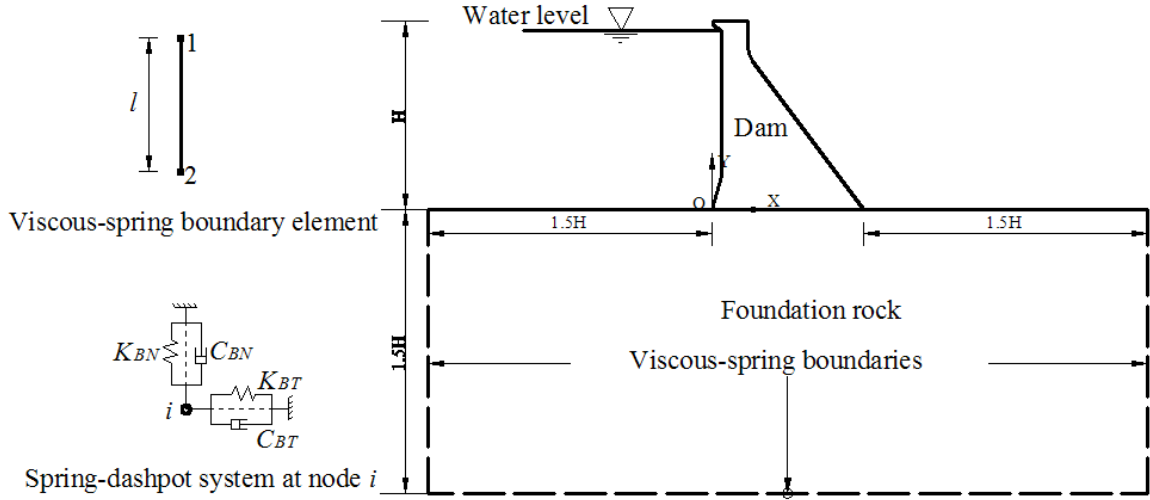


Fig.1 Viscous-spring boundary of dam-foundation system

The free-field stress σ_B^f is obtained by elastic theory (He *et al.*, 2010).

$$\begin{cases} \sigma_{xx} \\ \sigma_{yy} \\ \sigma_{xy} \end{cases} = \begin{bmatrix} \lambda + 2G & \lambda & 0 \\ \lambda & \lambda + 2G & 0 \\ 0 & 0 & G \end{bmatrix} \begin{cases} \frac{\partial u}{\partial x} \\ \frac{\partial v}{\partial y} \\ \frac{\partial u}{\partial y} + \frac{\partial v}{\partial x} \end{cases} \quad (8)$$

When P waves are vertically propagated from the bottom boundary, the boundary conditions are $u=0$ and $v = v_0(t)$. The free field displacement and velocity at height h are determined by the wave motion theory, which are composed of two parts, the incident wave and reflected wave,

$$\begin{cases} v = v_0(t - \frac{h}{c_p}) + v_0(t - \frac{2H-h}{c_p}) \\ \dot{v} = \dot{v}_0(t - \frac{h}{c_p}) + \dot{v}_0(t - \frac{2H-h}{c_p}) \\ \frac{\partial v}{\partial y} = -\frac{1}{c_p} \left[\dot{v}_0(t - \frac{h}{c_p}) - \dot{v}_0(t - \frac{2H-h}{c_p}) \right] \end{cases} \quad (9)$$

where H is the distance from the bottom boundary to the free surface.

Substituting Eq. (9) into Eq. (8) and taking into account the boundary conditions $h=0$ and $\mathbf{n}=[0 \ -1]^T$, the free field stress σ_B^f is calculated as

$$\begin{Bmatrix} \sigma_{xx} \\ \sigma_{yy} \\ \sigma_{xy} \end{Bmatrix} = \begin{Bmatrix} 0 \\ \rho c_p^2 \frac{\partial v}{\partial y} \\ 0 \end{Bmatrix} = \begin{Bmatrix} 0 \\ -\rho c_p \left[\dot{v}_0(t - \frac{h}{c_p}) - \dot{v}_0(t - \frac{2H-h}{c_p}) \right] \\ 0 \end{Bmatrix} \quad (10)$$

Substituting Eq. (9) and (10) into Eq. (7), the equivalent load F_B can be expressed as

$$\begin{aligned} \begin{Bmatrix} F_{Bx} \\ F_{By} \end{Bmatrix} &= \begin{bmatrix} K_{BT} & 0 \\ 0 & K_{BN} \end{bmatrix} \begin{Bmatrix} 0 \\ v_0(t - \frac{h}{c_p}) + v_0(t - \frac{2H-h}{c_p}) \end{Bmatrix} + \begin{bmatrix} C_{BT} & 0 \\ 0 & C_{BN} \end{bmatrix} \begin{Bmatrix} 0 \\ \dot{v}_0(t - \frac{h}{c_p}) + \dot{v}_0(t - \frac{2H-h}{c_p}) \end{Bmatrix} \\ &+ \begin{Bmatrix} 0 \\ \rho c_p \left[\dot{v}_0(t - \frac{h}{c_p}) - \dot{v}_0(t - \frac{2H-h}{c_p}) \right] \end{Bmatrix} \\ &= \begin{Bmatrix} 0 \\ K_{BN} \left[v_0(t) + v_0(t - \frac{2H}{c_p}) \right] + C_{BN} \left[\dot{v}_0(t) + \dot{v}_0(t - \frac{2H}{c_p}) \right] + \rho c_p \left[\dot{v}_0(t) - \dot{v}_0(t - \frac{2H}{c_p}) \right] \end{Bmatrix} \end{aligned} \quad (11)$$

When the shear waves are vertically propagated from the bottom boundary, the boundary conditions are $u=u_0(t)$ and $v=0$. The equivalent loads F_B are derived by the analogous method.

$$\begin{Bmatrix} F_{Bx} \\ F_{By} \end{Bmatrix} = \begin{Bmatrix} K_{BT} \left[u_0(t) + u_0(t - \frac{2H}{c_s}) \right] + C_{BT} \left[\dot{u}_0(t) + \dot{u}_0(t - \frac{2H}{c_s}) \right] + \rho c_s \left[\dot{u}_0(t) - \dot{u}_0(t - \frac{2H}{c_s}) \right] \\ 0 \end{Bmatrix} \quad (12)$$

The corresponding equivalent force loads F_B of the free field stress at the lateral boundaries (Fig. 1) of the gravity dam-foundation system can also be easily derived by the aforementioned method.

The viscous-spring boundary element is implemented by the element type COMBIN14 in the commercial finite element software ANSYS 10.0. A macro file for the corresponding wave input is created using ANSYS Parametric Design Language (APDL).

Numerical example

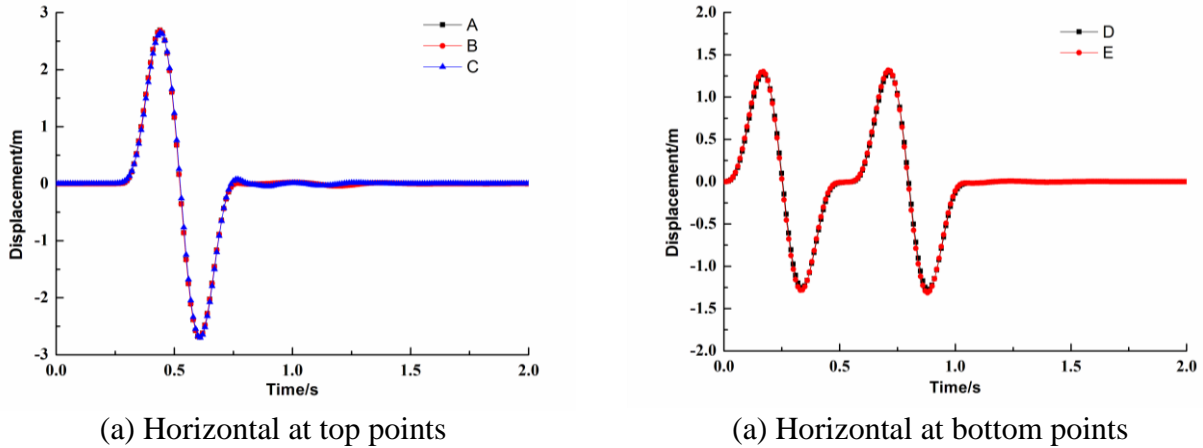
In order to verify the correctness of the viscous-spring boundary element and its wave input programme, an elastic half-space is studied. A vertically propagating S wave is analyzed, and the displacement equation of the input wave is

$$u(t) = \begin{cases} \sin(4\pi t) - 0.5 \sin(8\pi t) & 0 \leq t \leq 0.5 \\ 0 & t > 0.5 \end{cases} \quad (13)$$

The elastic medium has the following parameters: modulus of elasticity $E=13.23$ GPa, Poisson's ratio $\mu=0.25$, mass density $\rho=2700$ kg/m³, S-wave velocity $c_s=1400.0$ m/s, and P-wave velocity $c_p=2425$ m/s. The semi-unbounded foundation with an area $762 \text{ m} \times 381 \text{ m}$ is analyzed, and four-node solid elements with 2×2 Gauss integration points are adopted. The mesh size is 19.05 m , and there are a total of 800 elements and 946 nodes, of which there are 81 viscous-spring boundary elements on the bottom and lateral boundaries. The total calculation time is 2s. The fixed time step 0.005s is selected.

The horizontal displacement time histories of the free and bottom surfaces are shown in Fig. 2. It could clearly be seen that the maximum displacement of the free surface is nearly twice the corresponding amplitude of the input wave. Additionally, the displacements of the bottom points are basically the same, with the first half of the displacement time history showing the input wave

and the latter part of the displacement time history showing the reflection wave. The results are consistent with the theoretical solutions of wave motion. Therefore, it is concluded that the viscous-spring boundary element and wave input program are accurate.



(a) Horizontal at top points (a) Horizontal at bottom points
Fig.2 Time histories of the top and bottom displacements

Engineering Application

The seismic response analysis of the Longtan gravity dam is selected as an engineering example. The Longtan hydropower station is mainly built for power generation in the upper reaches of the Hongshui River, China. The dam is a roller-compacted concrete (RCC) gravity dam with a crest elevation of 406.50 m. The maximum dam height is 216.50 m with a crest length of 849.44 m and downstream slope ratio of 1:0.75. The upstream slope ratio below the height of 270.00 m is 1:0.25. According to the research results from the Institute of Geology, State Seismological Bureau of China, the basic seismic intensity of the dam site is 7 degrees. The designed peak horizontal ground acceleration of the dam site is 0.2g.

The retaining water monolith of the dam as shown in Fig.3 is investigated in this paper. The four-node plane strain quadrilateral isoparametric elements with 2×2 Gauss integration are adopted. The system is discretized with 4562 elements and 4737 nodes including 175 viscous-spring boundary elements on the bottom and lateral boundaries. Finite element discretization of the dam is shown in Fig.4.

The concrete has the following parameters: modulus of elasticity $E_c=19.6$ GPa, Poisson's ratio $\mu_c=0.167$, the unit weight $\gamma_c=24.0$ kN/m³, and the damping ratio $\zeta=0.08$. The rock mass has the following parameters: modulus of elasticity $E_r=13.2$ GPa, Poisson's ratio $\mu_r=0.25$, the unit weight $\gamma_r=27.0$ kN/m³. The dynamic elastic modulus of concrete and rock are taken as 1.3 times the corresponding static modulus (SETC, 2001). The artificial acceleration time history is simulated according to the design response spectrum (SETC, 2001). The total calculation time is 20s, and the fixed time step is $\Delta t=0.01$ s. The input accelerations and response spectrum are shown in Fig.5.

Two earthquake input mechanisms are considered in this paper. The first one is the massless foundation model proposed by Clough. The foundation is considered massless. The dynamic load is uniformly applied to the dam body by inertia force. The second one is the viscous-spring boundary model. The dynamic loads are transformed into the bottom and lateral's equivalent nodal loads by Eq. (10), (11) and are applied to the truncated boundary. According to the numerical example in Section 3, the input wave of the bottom boundary would amplify nearly 1 time on the free surface. Thus, the input earthquake wave in the viscous-spring boundary model is taken as 0.5 times the

corresponding amplitude of Fig.5.

The peak values of the displacement and stress at key points are shown in Table 1. The comparisons of the displacements are shown in Fig.6. The comparisons of stresses at the key parts are shown in Fig.7. The results show that the peak values of dam's dynamic responses are reduced by 4%~38% compared to the massless foundation model. The structural dynamic responses are overestimated to some extent utilizing the traditional massless model. The radiation damping effect of infinite foundation has a great influence to the structure's dynamic responses, and is very necessary to be considered.

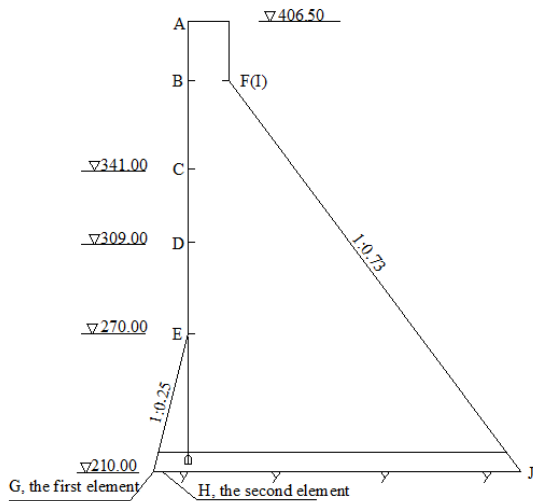


Fig.3 The retaining water section

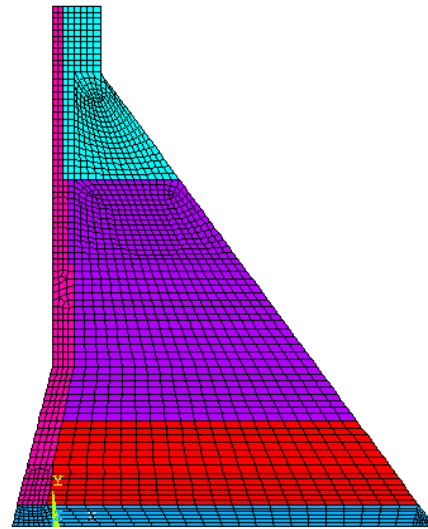


Fig.4 FE Mesh of the dam

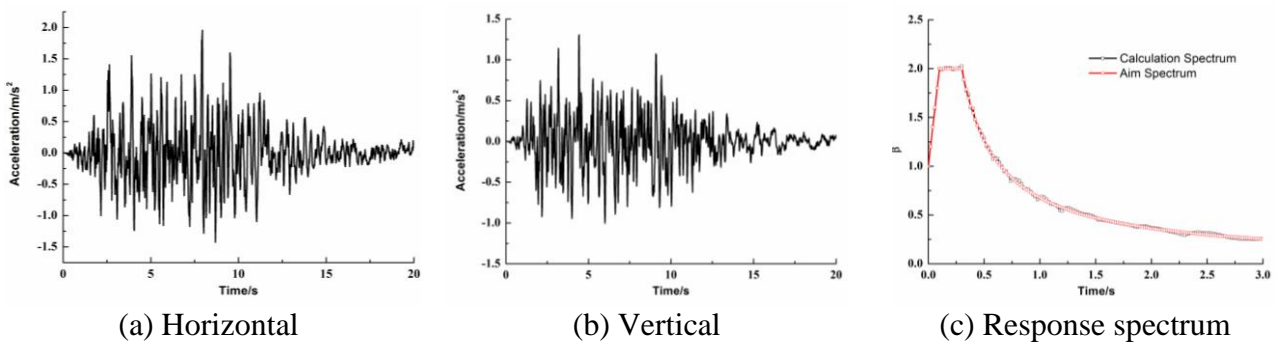


Fig.5 The input accelerations and response spectrum

Table 1 Comparisons of displacements and stresses at key points

Feature points of the dam section	Massless foundation model	Viscous-spring boundary	Relative error
Horizontal displacements at point A U_x /cm	5.86	4.11	29.9%
Vertical displacements at point A U_y /cm	1.47	0.92	37.4%
Horizontal displacement at point F U_x /cm	4.09	2.80	31.5%
First principal stresses at point E σ_1 /MPa	2.38	1.51	36.6%
First principal stresses at point F σ_1 /MPa	2.32	2.23	3.9%
First principal stresses at point G σ_1 /MPa	2.60	2.44	6.2%

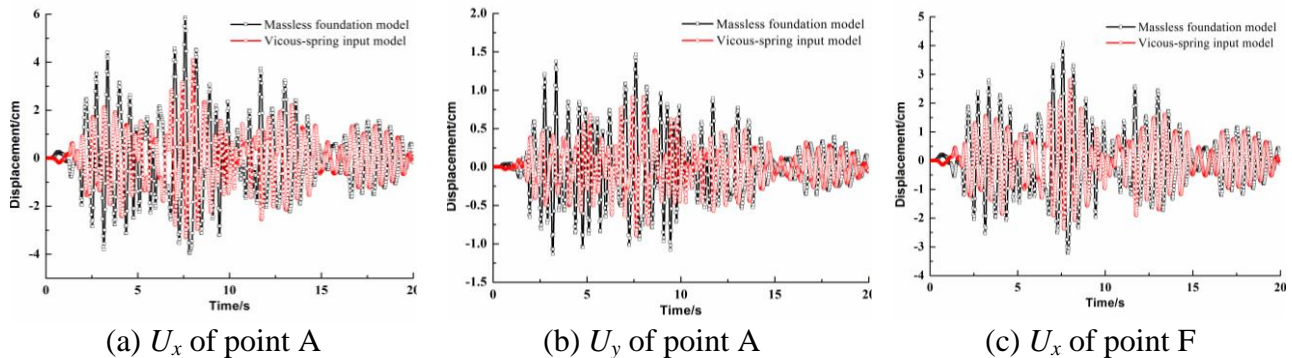


Fig.6 Comparisons of the displacements for the different seismic input models

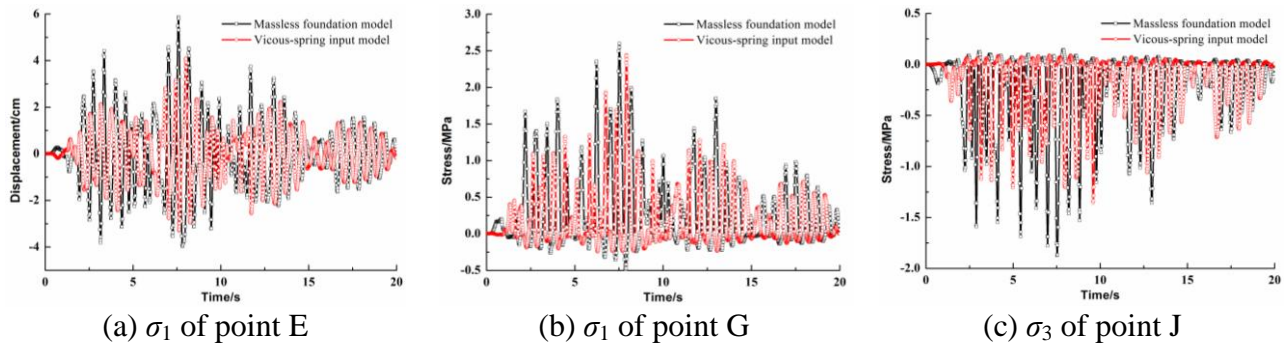


Fig.7 Comparison of the stresses for the different seismic input models

Conclusion

Two different earthquake input models are presented in the paper, i.e. massless foundation model and viscous-spring boundary. Based on the commercial nonlinear finite element code ANSYS, the user element subroutine of the viscous-spring boundary is implemented. The correctness of the viscous-spring boundary and its wave input model are validated by a numerical example. Finally, the viscous-spring boundary and wave input model are applied to the seismic analysis of the Longtan gravity dam-foundation system. The results show that the peak values of dam's dynamic responses are reduced by 4%~38% compared to the massless foundation model. The structural dynamic responses are overestimated to some extent utilizing the traditional massless model. The radiation damping effect of infinite foundation has a great influence to the structure's dynamic responses, and is very necessary to be considered.

References

- Clough, R.W. (1980), Nonlinear mechanisms in the seismic response of arch dams. Proceedings of International Research Conference on Earthquake Engineering, Skopje, Yugoslavia.
- Lysmer, J. and Kuhlemeyer, R. L. (1969), Finite dynamic model for infinite media. *Journal of Engineering Mechanics, ASCE*, 95, 759–877.
- Deeks, A. J. and Randolph, M. F. (1994), Axisymmetric time-domain transmitting boundaries. *Journal of Engineering Mechanics Division, ASCE*, 120, 25–42.
- Liu, J. B., Du, Y. X. and Du, X. L. (2006), 3D viscous-spring artificial boundary in time domain. *Earthquake Engineering and Engineering Vibration*, 5, 93–102.
- Liao, Z. P., Wong, H. L. and Yang B. (1984), A transmitting boundary for transient wave analyses. *Scientia Sinica Mathematica*, 27, 1063–1076.
- Wolf, J. P. and Song, C. (1996), *Finite-element modeling of unbounded media*. Wiley: New York.

- Du, X. L., Zhao, M. and Wang, J. T. (2006), A stress artificial boundary in FEA for near-field wave problem. *Chinese Journal of Theoretical and Applied Mechanics*, 38(1), 49–56. (in Chinese)
- He, J. T., Ma, H. F., Zhang B. Y. and Chen, H. Q. (2010), Method and realization of seismic motion input of viscous-spring boundary. *Journal of Hydraulic Engineering*, 41(8), 960–969. (in Chinese)
- State Economic and Trade Commission (SETC) (2001), *Specifications for Seismic Design of Hydraulic Structures DL 5073–2000*, China. (in Chinese)